Controlled Living Polymerization of Carbodiimides Using Versatile, Air-Stable Nickel(II) Initiators: Facile Incorporation of Helical, Rod-like Materials

ARTICLE *in* MACROMOLECULES · JUNE 2014

Impact Factor: 5.8 · DOI: 10.1021/ma5009429

6 AUTHORS, INCLUDING:

James F Reuther
University of Texas at Austin
9 PUBLICATIONS **50** CITATIONS
SEE PROFILE

Mahesh Bhatt
Lawrence Berkeley National Laboratory
19 PUBLICATIONS **215** CITATIONS
SEE PROFILE

Raymond Campos
University of Texas at Dallas
11 PUBLICATIONS **84** CITATIONS
SEE PROFILE

Bruce Novak
University of Texas at Dallas
135 PUBLICATIONS **5,654** CITATIONS
SEE PROFILE

Macromolecules

Article

pubs.acs.org/Macromolecules

Controlled Living Polymerization of Carbodiimides Using Versatile, Air-Stable Nickel(II) Initiators: Facile Incorporation of Helical, Rod-like Materials

James F. Reuther,[†,‡] Mahesh P. Bhatt,[†] Gonglu Tian,[‡] Benjamin L. Batchelor,[†] Raymond Campos,[†] and Bruce M. Novak*[,†]

[†]Department of Chemistry and Alan G. MacDiarmid NanoTech Institute, University of Texas Dallas, Richardson, Texas 75080, United States

[‡]Department of Chemistry, North Carolina State University, Raleigh, North Carolina 27695, United States

Supporting Information

ABSTRACT: The new polymerization of carbodiimides using two, simple [bis(triphenylphosphino)aryl]nickel(II) bromide complexes has been discovered to occur in a controlled, living fashion. These initiators are substantially more air and moisture stable compared to their titanium(IV) counterparts making them significantly easier to synthesize, purify, and utilize. The polymerization is initiated via aryl ligand transfer to the electrophilic center carbon of the carbodiimide. Sequential insertions of the carbodiimide π-bond into the nickel−nitrogen amidinate coordination bond propagates the polymer chain in a living chain growth manner as evident by the linear relationship in the plots of percent conversion vs M_n, $\ln([M]_o/[M])$ vs time, and monomer: initiator ratio vs M_n. The transferred aryl ligand was confirmed to be appended to the terminus of the polymer chain by MALDI−TOF and ^{19}F NMR. This added control element offers new opportunities to end functionalize rigid-rod, helical polycarbodiimides. This new technique also provides the ability to generate the active Ni(II) initiation sites on potentially any aryl bromide species for the facile incorporation of rod-like, helical polycarbodiimides into such systems as block copolymers, graft copolymer, polymer functionalized surfaces, etc. To demonstrate this, poly(4-bromostyrene) was employed as a polymer-supported aryl bromide source to generate the active [bis(triphenylphosphino)aryl]nickel(II) bromide macroinitiator. The "grafting from" reaction was then carried out upon addition of the chiral (*S*)-PEMC monomer forming the excess single-handed helical polycarbodiimide appended graft copolymer. The morphology of this novel polymer system was studied using TMAFM, revealing nanofibular aggregation behavior when spin coated from dilute $CHCl_3$ solutions.

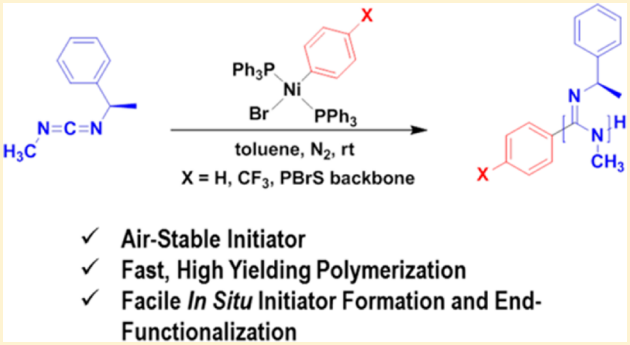

INTRODUCTION

Traditional cross coupling polymerizations such as Sonogashira,[1] Suzuki,[2] Heck,[3] and Negishi[4] polymerizations occur through step-growth mechanisms offering limited control over molecular weight and copolymer composition. However, a plethora of new, controlled living transition metal-mediated polymerization techniques have surfaced in recent years offering new opportunities to polymerize a variety of monomers with controlled molecular weights (MW) and copolymer composition. Several examples include atom transfer radical polymerizations (ATRP),[5,6] ring-opening metathesis polymerizations (ROMP),[7,8] titanium(IV) mediated polymerization of isocyanates/carbodiimides,[9,10] nickel(II) mediated polymerization of isocyanides,[11] palladium(II) mediated polymerization of isocyanides,[12] and nickel(II) mediated Kumada chain-growth polycondensation of arylenes (e.g., phenylenes,[13,14] pyrolle,[14] thiophenes,[13−15] fluorenes,[16] selenophenes,[17] etc.).

The added control in living polymerizations provides the opportunity to specifically end functionalize macromolecules using functional initiators. This feature also allows for the formation of complex macromolecular architectures such as star copolymers,[18] graft copolymers,[19] block copolymers,[20] hyperbranched/dentritic polymer systems,[21] hybrid organic−inorganic polymers,[22] etc. The end group functionalization of polythiophenes has been reported by Smeets et al. when they employed several functional aryl(bromo) nickel(II) initiators to end group functionalize polythiophenes with protected alkyne and alcohol groups located at the 4-position of the η^1-coordinated aryl ligand.[20] The negatively charged, aryl ligand is transferred to the first monomer unit via transmetalation which then allows for propagation to occur. Khanduyeva et al. took this polymerization technique

Received: May 7, 2014
Revised: June 18, 2014

   dx.doi.org/10.1021/ma5009429 | Macromolecules XXXX, XXX, XXX−XXX

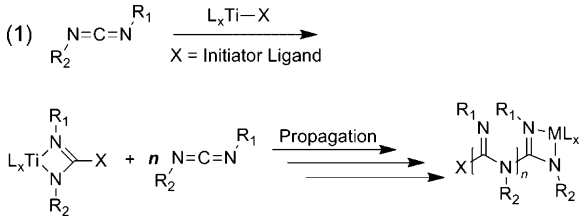

one step further by synthesizing silica-grafted nickel(II) macroinitiators from aryl bromide functionalized silica nanoparticles for the well-defined growth of poly(3-hexylthiophene) (P3HT) conjugated materials.[22]

In 1994, Goodwin and Novak reported the controlled polymerization of carbodiimide monomers with titanium(IV) initiators.[9] The polymerization was shown to occur through a reversible coordination−insertion mechanism where the reaction is first initiated upon insertion of one of the carbodiimide π-bonds into the M−X bond (eq 1). The initiator ligand X (typically an alkoxide or amine ligand bound to the Ti(IV) catalyst) is then transferred to the center carbon of the carbodiimide monomer forming a titanium amidinate complex. Propagation then ensues as additional carbodiimide monomer units insert into the amidinate complex extending the polymer chain in a living fashion. The resulting polymers possess a repeating amidine structure with two tunable pendant groups per repeat unit. Because of the steric interactions of adjacent side groups, these novel macromolecules adopt a stable, helical conformation in the solution and solid state and can be used in a wide range of applications including providing liquid crystallinity,[23,24] chiral sensing,[25] polymer catalyst supports,[26] and temperature/solvent controlled chiroptical switching.[27−30]

The air sensitivity and difficult synthesis of the titanium(IV) complexes provides significant challenges for the formation of functional initiators to end-group functionalize polycarbodiimides and offers little opportunities for the copolymerization of carbodiimides with different classes of monomers. For these reasons, alternative, air stable nickel(II) complexes, like those previously mentioned for the polymerization/end-group functionalization of polythiophenes, were hypothesized to be viable catalyst systems for the polymerization of carbodiimides due to the possibility of the negatively charged, η^1 aryl ligand acting as the necessary initiator ligand similar to that of the titanium(IV) systems. Herein, we report the synthesis of two, simple nickel(II) complexes and the controlled living polymerizations of carbodiimides using these versatile initiators. The aryl ligand transfer from the Ni(II) complex to become the chain end was confirmed by MALDI−TOF mass spectrometry and ^{19}F NMR spectroscopy. These complexes provide a facile route to end functionalize helical, liquid crystalline polycarbodiimides. Additionally, this new technique provides facile *in situ* catalyst formation upon activation of aryl bromides with Ni(COD)$_2$ and triphenylphosphine allowing for the design and incorporation of helical polycarbodiimides into a variety of complex architectures such as block, star, or graft copolymers. To demonstrate this, a monodisperse sample of poly(4-bromostyrene) (PBrS) synthesized via controlled RAFT polymerization techniques was employed as the aryl bromide source for *in situ* Ni(II) macroinitiator formation. Upon addition of *N*-(*S*)-1-phenylethyl-*N*′-methylcarbodiimide ((*S*)-PEMC) monomer, the chiral, helical polycarbodiimide chains propagate from the random coil PBrS creating a novel form of rod-*g*-coil copolymers. The thin-film morphology of this polymer was also studied here in by tapping-mode atomic force microscopy (TMAFM) revealing nanofibular aggregation behavior when spin-coated from dilute $CHCl_3$ solutions.

EXPERIMENTAL SECTION

Materials. All solvents, reagents, and reactants used for the synthesis of monomers were purchased from Sigma-Aldrich and used as received. The bis(cyclooctadiene) Ni(0) (Alfa Aesar, 99%), triphenylphosphine (Sigma-Aldrich, 99%), bromobenzene (Alfa Aesar, 99%), and 4-trifluoromethylbromobenzene (Alfa Aesar, 98%) used in the synthesis of **Cat-1** and **Cat-2** were also used as received. The toluene used in the synthesis of catalysts and polymers was vacuum distilled over CaH_2 into an oven-dried Schlenk flask equipped with 3 Å molecular sieves and stored in an N_2 atmosphere MBraun UNILAB glovebox prior to use. The 4-bromostyrene was distilled into an oven-dried Schlenk flask equipped with 3 Å molecular sieves prior to RAFT polymerization. The RAFT agent 2-cyano-2-propyldodecyltrithiocarbonate (Sigma-Aldrich) and AIBN (Sigma-Aldrich) were used as received.

Equipment. All NMR spectra (including ^{1}H, ^{13}C, ^{15}N, ^{19}F, and ^{31}P) were recorded on a Bruker AVANCE III 500 MHz NMR spectrometer. All FTIR spectra were collected on Thermo Scientific Nicolet 380 ATR-FTIR spectrometer. Specific optical rotations of chiral polymers were measured using a JASCO P-1010 polarimeter (435 nm, l = 10.0 cm) at room temperature in dilute solution ($CHCl_3$, c = 2.00 mg/mL). Vibrational circular dichroism (VCD) spectra were collected using a BioTools ChiralIR-2X VCD spectrometer in deuterated chloroform (c = 25.0 mg/mL l = 50.0 μm). Matix-assisted laser desorption/ionization time-of-flight (MALDI−TOF) mass spectrometry of polymers was carried out using a Shimadzu Axima Confidence MALDI−TOF mass spec using dithranol (Sigma-Aldrich) as a matrix, $CHCl_3$ as a solvent, and no salt added. The progress of the polymerizations were monitored via GC/MS on an Agilent 6890−5973 GC−MS workstation equipped with a Hewlett-Packard fused silica capillary column cross-linked with 5% phenylmethyl siloxane. All GC/MS analyses were conducted via the same method: injector and detector temperature, 250 °C; initial temperature, 70 °C; temperature ramp, 10 °C/min; final temperature, 280 °C. TMAFM was employed to investigate the thin-film morphology of the graft copolymer using a Nanoscope IV-Multimode Veeco instrument equipped with an E-type vertical engage scanner.

Characterization. All NMR spectra were recorded in either $CDCl_3$ (Sigma-Aldrich), DMSO-d_6 (Sigma-Aldrich), or toluene-d_8 (Sigma-Aldrich). ^{1}H NMR spectra were referenced internally to tetramethylsilane (TMS) set to 0 ppm; ^{15}N NMR spectra were referenced externally to ^{15}N-benzamide set to 0 ppm; ^{19}F NMR spectra were referenced externally to trichlorofluoromethane ($CFCl_3$) set to 0 ppm; ^{31}P NMR spectra were referenced externally to 85% phosphoric acid (H_3PO_4) set to 0 ppm. The procedure for MALDI−TOF analysis of polymers is as follows: each polymer solution (20 μL; 5.0 mg/mL) was mixed with the dithranol solution (200 μL; 15.0 mg/mL) in a clean Eppendorf tube. Proteomass ACTH Fragment 18−39 (exact mass = 2464.1989 Da), Proteomass Insulin Chain B oxidized (exact mass = 3493.6513 Da), and Proteomass Insulin (exact mass = 5729.6087 Da) were purchased from Sigma-Aldrich and used to calibrate externally for all MALDI−TOF mass spec collected. All MALDI−TOF MS reported for samples and calibrants were analyzed in linear mode. Thin-films for TMAFM were prepared by passing dilute polymer solutions (5.0 mg/mL; $CHCl_3$) through 0.45 μm PTFE syringe filters, spin-casting on silicon wafer (Wafer World) spun at 1000 rpm for 30 s and annealed in $CHCl_3$ vapor for 24 h. The images were recorded at room temperature using silicon cantilever probes with a nominal spring constant of 42 N/m and resonance frequency of 320 kHz. The images reported herein were acquired at 0.996 Hz scan frequency in 10 and 15 μm scan areas.

Molecular Weight Determination. Molecular weights of the synthesized polymers were measured by Size Exclusion Chromatography (SEC) analysis on a Viscotek VE 3580 system equipped with ViscoGEL columns (GMHHR-M), connected to a refractive index (RI) detectors. GPC solvent/sample module (GPCmax) was used with HPLC grade chloroform as the eluent and calibration was based

dx.doi.org/10.1021/ma5009429 | *Macromolecules* XXXX, XXX, XXX−XXX

on polystyrene standards. Running conditions for SEC analysis were as follows: flow rate = 1.0 mL/min, injector volume =100 μL, detector temperature = 30 °C, column temperature = 35 °C. All the polymers samples were dissolved in chloroform, and the solutions were filtered through PTFE filters (0.45 μm) prior to injection. For comparison, the MWs of several polymer systems were also run on a Shimadzu Prominence Modular HPLC/GPC system connected to a refractive index (RI) detector relative to a polystyrene standard. A two-column system was employed consisting of an Agilent Mixed-E and Mixed-C column. The polymer samples were dissolved in HPLC grade chloroform (ca. 1.8 mg/mL) with 0.5% (v/v) *N*,*N*-dimethylethylenediamine added to the sample. The samples were passed through 0.45 μm PTFE filter prior to injection. The flow rate for all samples was 1.0 mL/min, and the injection volume was 50 μL.

Synthesis of Urea Precursors. Most ureas were synthesized following literature procedures previously reported.[9,31] The synthesis and characterization of all new ureas can be found in the Supporting Information.

Synthesis of Carbodiimide Monomers. The general procedure for all carbodiimide monomers is as follows: An oven-dried 500 mL round-bottom flask was purged with N_2 for 30 min and cooled to 0 °C in an ice bath. Dibromotriphenylphosphorane (PPh_3Br_2, 1.2 equiv) was then added to the purged flask along with ∼10 mL of dry dichloromethane (DCM). Triethylamine (TEA, 2.5 equiv) was then added slowly to the cool solution and the resulting vapors were allowed to dissipate prior to addition of the urea/thiourea (1.0 equiv). The reaction mixture was then allowed to stir at 0 °C and monitored by the appearance of N═C═N stretch at 2100−2200 cm^{-1} in the IR spectrum. Upon completion, typically ∼1−4 h, the reaction was quenched with ∼250 mL of hexanes and the resulting precipitate was filtered. The filtrate was then concentrated by rotatory evaporation and the quenching process was repeated twice more to remove the majority of byproducts (triphenylphosphine oxide/sulfide and triethylammonium bromide). The remaining purification varied from monomer to monomer. The purification and characterization of **Mono-1** and **Mono-2** have been previously reported.[9,31] **Mono-3** was further purified via column chromatography using DCM as the mobile phase and dried under high vacuum prior to polymerization. The characterization of **Mono-3** (including ^{1}H NMR, ^{13}C NMR, FTIR, and HRMS-ESI) can be found in the Supporting Information.

Synthesis of Ni(II) Initiators. Both initiators were synthesized following the same procedure outlined below. The synthesis and characterization of **Cat-1** has been previously reported in the literature[32,33] but via a different method then that reported herein. In an N_2 atmosphere glovebox, an oven-dried vial was charged with triphenylphosphine (PPh_3; 3.0 equiv), the corresponding aryl bromide (bromobenzene for **Cat-1** and 4-trifluoromethylbromobenzene for **Cat-2**; 1.5 equiv) and ∼3 mL of dry toluene. For **Cat-2**, catalytic amount of benzonitrile (PhCN; 0.1 equiv) was added to the mixture to aid in the oxidative addition of the aryl bromide onto the metal center as explained by Hartwig et al.[34] To the stirring solution, the bis(1,5-cyclooctadiene)nickel(0) ($Ni(COD)_2$) was added with an additional 0.5 mL of dry toluene, and the mixture was allowed to stir at room temperature for 30 min. The reaction vial was then removed from the glovebox and ∼15 mL of hexanes was added to the mixture precipitating the product. The suspension was allowed to stir for 2 h; the solid was filtered, and washed with 100 mL of hexanes, 100 mL of methanol, and 50 mL of 2-propanol. The pure products were then collected as yellow-orange solids and dried under high vacuum.

Polymerization of Carbodiimides. In an inert N_2 atmosphere glovebox, an oven-dried vial was charged with the corresponding amount of monomer along with 2−5 mL of dry toluene. The initiator was then added directly into the stirring mixture and allowed to stir for 12 h. The reaction vial was then removed from the glovebox and the product was precipitated from 100 mL of 1.0% (v/v) 1,8-diazabicyclo[2.5.0]undec-7-ene (DBU) solution in methanol. The DBU is added to the precipitating solvent in order to aid in the extraction of the residual nickel in the system. If the color associated with residual catalyst persists after the first precipitation, the polymer was redissolved in the minimal amount of $CHCl_3$ and precipitated again. For all cases studied, this is a sufficient method to remove the vast majority nickel from the system. The pure polymer was then isolated by filtration as a white solid, washed with 100 mL of methanol, and dried under high vacuum. The specific amounts of reagents, yields, ^{1}H NMR, FTIR, MW, etc. for all synthesized polymer can be found in the Supporting Information.

Polymerization Kinetics. Both initiators were studied using the following conditions: In an inert N_2 atmosphere glovebox, the (*R*)-PEMC monomer (**Mono-2(*R*)**; 3.77 mmol) and the internal standard 1,4-dimethoxybenzene (DMB; 0.938 mmol) were added to an oven-dried vial along with 4.0 mL of dry toluene. The corresponding initiator (18.8 μmol; 200:1 Mono:Cat ratio) was then added to the stirring mixture along with 1.0 mL of dry toluene. The progress of the polymerization was monitored by taking aliquots (∼0.2 mL) of the polymerization reaction at different time intervals and then quenching into 5 mL of MeOH. The concentration of monomer was monitored relative to DMB internal standard by GC−MS in order to measure percent conversion and $\ln([M]_o/[M])$. The polymer precipitate was filtered, washed with 50 mL methanol, and dried under high vacuum. The polymer was then redissolved in 1.0 M *N*,*N*-dimethylethylenediamine $CHCl_3$ solution and the molecular weight was determined by SEC. The *N*,*N*-dimethylethylenediamine additive is added to the injection solution in order to reduce the affinity of polycarbodiimides with the SEC stationary phase.

"Grafting-From" Poly(4-bromostyrene). The poly(4-bromostyrene) was synthesized using the previously reported RAFT polymerization of 4-bromostyrene in the presence of 2-cyano-2-propyldodecyltrithiocarbonate (RAFT agent) and AIBN as an initiator.[35] In an N_2 atmosphere glovebox, an oven-dried vial was charged with poly(4-bromostyrene) (0.4078 g; 2.23 mmol of repeat units), triphenylphosphine (0.5302 g; 2.02 mmol) and 5.0 mL of dry toluene. The $Ni(COD)_2$ (0.1356 g; 0.493 mmol) was then added to the stirring solution and the reaction was allowed to proceed for ∼1 h monitoring the formation of the active initiation site by ^{31}P NMR. The (*S*)-PEMC monomer (1.040 g; 6.49 mmol) was then added to the solution and the graft copolymerization was allowed to react for an additional 8 h. Upon completion, the copolymer product was precipitated in MeOH/1.0 vol. % DBU, collected by filtration as a beige solid, and dried under high vacuum overnight. The yields, ^{1}H NMR, FTIR, VCD, DSC, and TGA data for the graft copolymer can be found in the Supporting Information.

RESULTS AND DISCUSSION

Oxidative addition of bis(1,5-cyclooctadiene) nickel(0) with aryl bromides in the presence of triphenylphosphine yields square planar, trans-substituted bis(triphenylphosphino)aryl nickel(II) bromide complexes (Scheme 1). Both bis(triphenylphosphino)-phenyl nickel(II) bromide (**Cat-1**) and bis(triphenylphosphino)-(4-trifluoromethylphenyl) nickel(II) bromide (**Cat-2**) were synthesized for subsequent polymerizations of carbodiimide monomers. Upon formation, both catalysts are air and moisture stable in the solid state providing substantially easier synthesis procedures then their titanium(IV) counterparts. However, these complexes, in the absence of monomer, quickly decompose via disproportionation (ca. 30 min) in solution to form colloidal Ni(0), Ni(I)Br, free PPh_3, and the corresponding, coupled biaryl species making the solution characterization of both **Cat-1** and **Cat-2** somewhat limited.[20] In order to characterize each complex by NMR, the compounds had to be dissolved in dry, deuterated $CDCl_3$ and immediately transferred to the instrument. ^{1}H NMR, ^{31}P NMR, and ^{19}F NMR (for **Cat-2** only; see Experimental Section) were successfully performed without significant decomposition but the longer times necessary for ^{13}C NMR analysis allowed for significant decomposition, making it very difficult to obtain suitable spectra.

The initial polymerization using **Cat-1** as an initiator was successfully accomplished on the ^{15}N-labeled ^{15}*N*-hexyl-*N*-phenylcarbodiimide (**Mono-1**) (ca. [**Mono-1**]/[**Cat-1**] = 48). Recently,

dx.doi.org/10.1021/ma5009429 | *Macromolecules* XXXX, XXX, XXX−XXX

Scheme 1. Synthesis of Nickel(II) Initiators Cat-1 and Cat-2 and Applied Polymerizations of Various Carbodiimide Monomers Forming High MW Liquid Crystalline Macromolecules

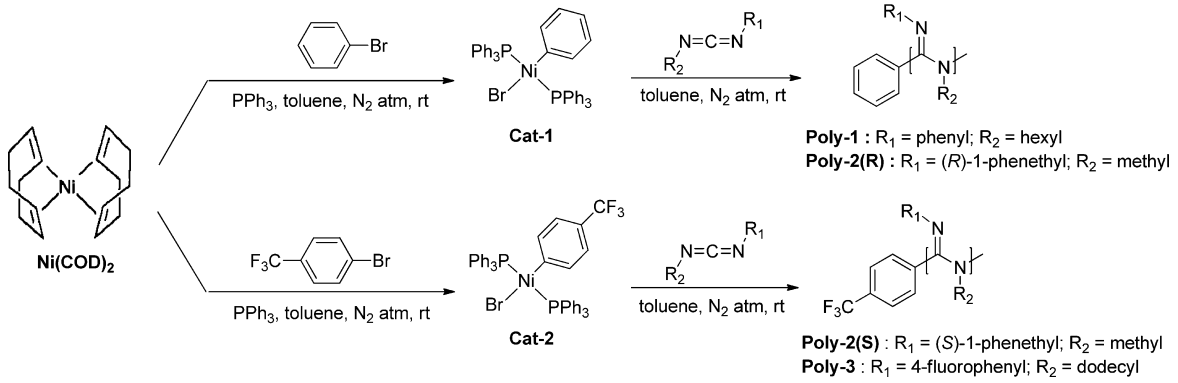

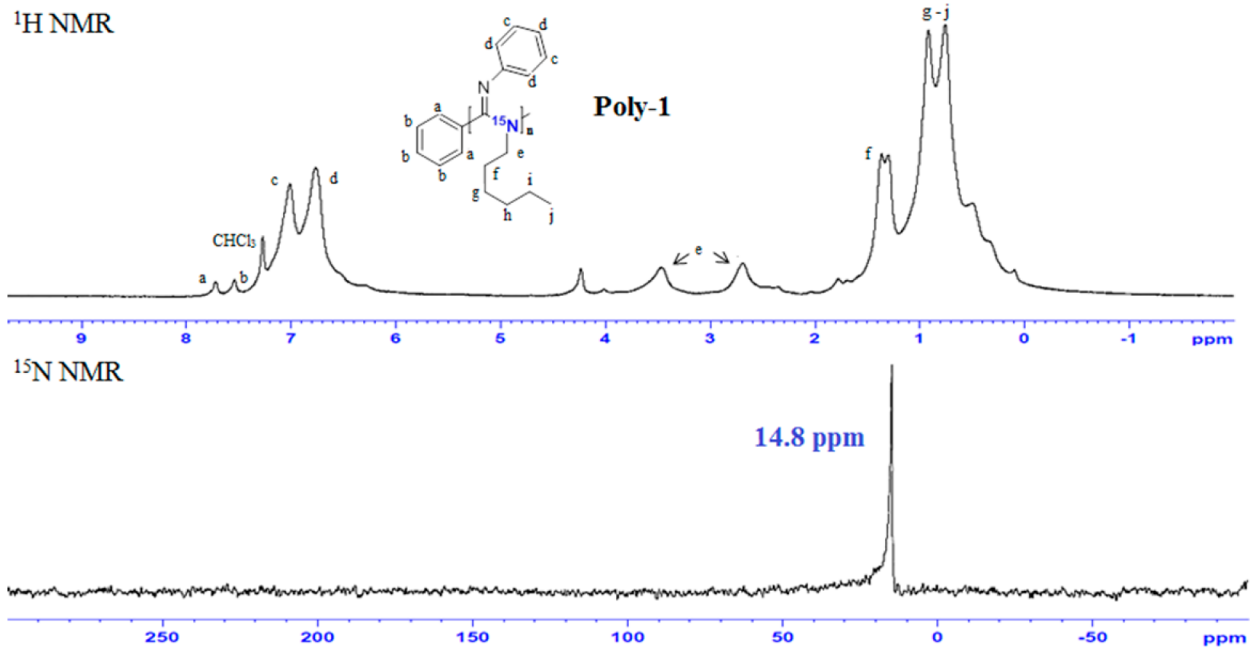

Figure 1. ^{1}H NMR and ^{15}N NMR spectra of ^{15}N-labeled **Poly-1** clearly showing the phenyl end group and the formation of a single regioisomer upon polymerization with **Cat-1**.

we employed the ^{15}N-isotope enrichment of several polycarbodiimides and subsequent ^{15}N NMR analysis to unambiguously determine the regioregularity of these polymers formed from Ti(IV) complexes.[31,36] The resulting polymers were shown to be completely regioregular when incorporating two sterically inequivalent pendant groups, i.e. the phenyl and hexyl side groups, with the more sterically bulky group located on the C═N imine nitrogen in all cases studied. **Mono-1** was synthesized using the same protocol as previously reported and was polymerized to determine if the same regioisomer is formed upon polymerization with nickel(II) complexes. The resulting poly(^{15}*N*-hexyl-*N*-phenylcarbodiimide) (**Poly-1**) was isolated with an 85% yield and was then characterized by ^{1}H and ^{15}N NMR (Figure 1) spectroscopy. The ^{15}N NMR spectrum of **Poly-1** displayed a single peak at 14.8 ppm confirming that the polymer is indeed regioregular with the hexyl pendant group only being incorporated onto the backbone amine nitrogen. The phenyl end-group of the polymer is also clearly visible in the ^{1}H NMR spectrum with resonant signals at 7.71 and 7.54 ppm suggesting that the negatively charged, η^{1} aryl ligand is transferred to the first carbodiimide monomer unit to initiate the polymerization. This makes these nickel(II) catalysts an attractive alternative to form end-group functionalized, liquid crystalline polycarbodiimides. As expected, the methylene unit directly attached to the polymer backbone from the hexyl side group is split into two chemical shifts due to the chirality of the helical backbone causing the protons to be diastereotopic.

Using the relative integration of these end group peaks with respect to the diastereotopic methylene protons from the hexyl chain, the molecular weight was calculated to be M_n = 4400 Da which matches closely to SEC results (ca. M_n = 5000 Da; PDI = 3.30). Polycarbodiimides have been reported to display a high affinity to the polystyrene substrate in the SEC columns causing abnormally large PDI values and skewed molecular weights.[9] One way to combat this problem is to add a small amount (~0.5 M) of an amine additive (*N*,*N*-dimethylethylenediamine in this case) to the mobile phase of the instrument to decrease the affinity of the polymer to the solid substrate. This method is helpful but does not completely remove the affinity of the

dx.doi.org/10.1021/ma5009429 | *Macromolecules* XXXX, XXX, XXX−XXX

polymer which is the reason for the slightly higher M_n value and unreliably large PDI observed.

For most applications of chiral, helical macromolecules, it is necessary to isolate predominantly single-handed helices upon polymerization. One way to bias the helicity of the polymer backbone is to employ chiral monomers resulting in optically active polymers with an excess single-handed screw sense. The chiral *N*-(*R*)-1-phenethyl-*N*′-methylcarbodiimide (**Mono-2(*R*)**; (*R*)-PEMC) and *N*-(*S*)-1-phenethyl-*N*′-methylcarbodiimide (**Mono-2(*S*)**; (*S*)-PEMC) were synthesized according to literature procedures.[23] The enantiomers of the monomers were polymerized using one of the two nickel initiators (i.e., **Cat-1** for **Mono-2(*R*)** and **Cat-2** for **Mono-2(*S*)**) and the kinetics of these polymerizations were monitored. The resulting polymers showed oppositely signed specific optical rotation values (ca. $[\alpha]^{25}_{435} = +51.2°$ and $[\alpha]^{25}_{435} = -49.4°$ respectively) verifying that the opposite handed helices are formed when the opposite enantiomer of monomer is utilized. In order to determine the exact handedness of the resulting helices, vibrational circular dichroism (VCD) analysis was undergone experimentally (Figure 2) and compared to previously reported, DFT calculated

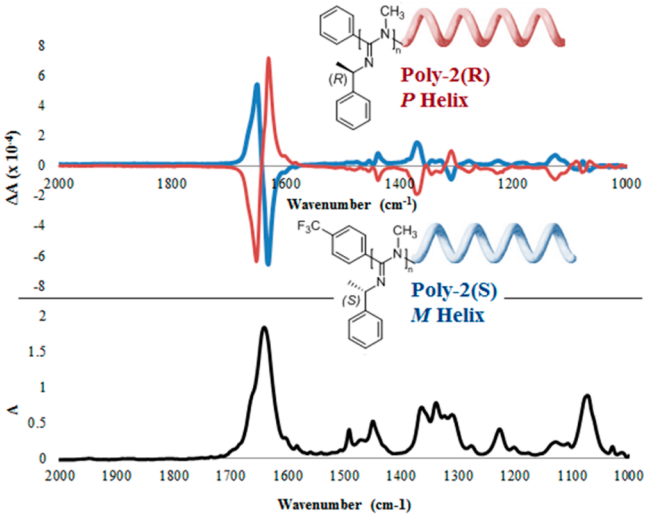

Figure 2. VCD (top) and IR (bottom) spectra of **Poly-2(*R*)** (red) and **Poly-2(*S*)** (blue) in $CDCl_3$ (c = 25.0 mg/mL) showing the formation of opposite handed helices through mirror-image VCD spectra.

VCD spectra of similar polycarbodiimides.[27,37,38] The resulting VCD spectra of **Poly-2(*R*)** and **Poly-2(*S*)** shows perfect mirror image spectra further substantiating the formation of opposite handed helices. The most important, diagnostic stretch in the spectra is the strong bisignate at 1649 and 1629 cm^{-1} corresponding to the C═N imine stretching mode of the polymer. When compared to the previously reported, theoretical spectra, we can assign the helical handedness of the polymers to left-handed (*M*-helix) for **Poly-2(*S*)** and right-handed (*P*-helix) for **Poly-2(*R*)**.

In order to classify this polymerization as living, we must show the absence of chain transfer and termination reactions. To determine this, the polymerization kinetics of **Mono-2** with **Cat-1** and **Cat-2** were monitored by GC/MS and GPC. Both polymerizations proceed very rapidly with ∼90% of the monomers being consumed within the first 90 min of both reactions. This new polymerization is significantly faster than the Ti(IV) initiators which reach ∼90% conversion of analogous monomers

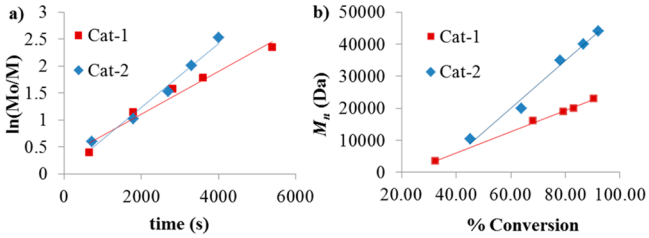

Figure 3. Polymerization kinetics of **Mono-2** with **Cat-1** and **Cat-2** shown in two plots: (a) time vs ln($[M_o]/[M]$) and (b) percent conversion vs M_n. The linear relationship in both plots provides further evidence of living character. (a) **Cat-1**: R^2 = 0.978. **Cat-2**: R^2 = 0.961. (b) **Cat-1**: R^2 = 0.998. **Cat-2**: R^2 = 0.980.

in ∼7 h.[9] To confirm or refute the presence of chain termination reactions, the reaction progress, i.e., the consumption of **Mono-2** during the polymerization reaction, was monitored by GC/MS as a function of time. A linear plot was constructed when plotting ln($[M]_o/[M]$) vs time confirming the absence of termination reactions (Figure 3a). Despite the difficulties determining MW by SEC for most polycarbodiimides, a linear relationship was observed in the plot of percent conversion vs M_n substantiating the absence of chain transfer reactions during the polymerization process when employing either **Cat-1** or **Cat-2** (Figure 3b). The PDI values of the resulting polymers were still somewhat inflated (ca. M_w/M_n = 2.7−3.3) by SEC which is uncommon for living polymerizations but, due to the aforementioned adhesion of polycarbodiimides to the SEC stationary phase, this is not unexpected.

Though the end groups are clearly visible in the ^{1}H NMR spectra of the polymers, additional evidence is necessary to determine the extent of end functionalization. MALDI−TOF mass spectrometry is one of the most accurate methods available for end group identification in polymer systems so **Poly-2(*R*)** was subject to this analysis to confirm the presence of the phenyl end groups on the terminus of the polymer chains. Additionally, we can use this method to unambiguously determine the functional group appended to the opposite terminus of the polymer. The polymerizations are quenched in 1.0% (v/v) DBU solution in methanol so the conventional hypothesis has been that the negatively charged amidinate ligand on the terminus of the polymer abstracts a proton from the methanol molecule upon work up. Examination of the MALDI−TOF MS of **Poly-2(*R*)** (Figure 4) confirms this hypothesis showing nearly exact masses (±1.0 Da) corresponding to the polymer chains of different molecular weight with a phenyl group and hydrogen appended to the termini. The overall molecular weight (MW) and polydispersity cannot be accurately determined using MALDI−TOF MS at this time due to difficulties observing MWs over ∼5000 Da. The low resolution and trailing amplitude of the m/z peaks (rather than the typical Gaussian distribution seen in MALDI−TOF MS of conventional polymer systems) suggests that only small portions of low MW polymer chains ablated with the matrix and reached the detector. Further optimization in sample preparation may be necessary to be able to observe the entire range of MWs.

The trifluoromethyl group at the 4-position of the η^1-aryl ligand on **Cat-2** provides an alternate opportunity to monitor the molecular weight using ^{19}F NMR. This is possible by incorporating a chemically distinct fluorine atom on one of the pendant groups of the polymer to provide a handle for end group analysis by the relative integration of the two chemical shifts. ^{19}F NMR provides enhanced signal separation and

dx.doi.org/10.1021/ma5009429 | *Macromolecules* XXXX, XXX, XXX−XXX

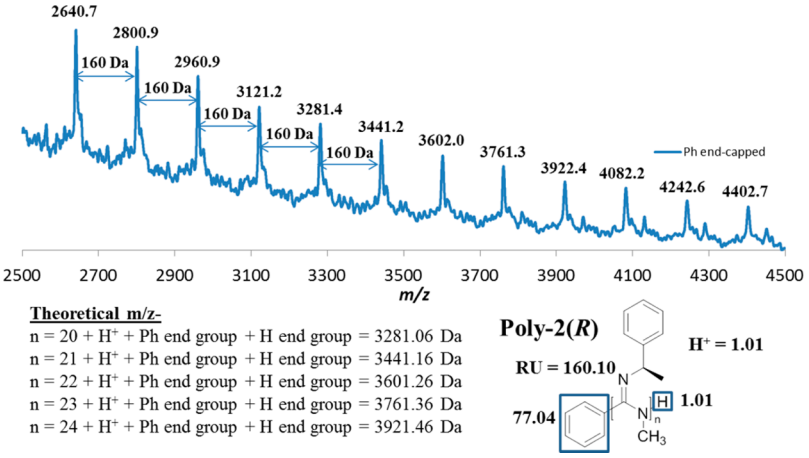

Figure 4. MALDI–TOF mass spec of **Poly-2(*R*)** showing a high degree of phenyl end group incorporation via polymerizations initiated by **Cat-1**. The second end group was also confirmed to be a hydrogen due to abstraction of a proton from methanol solvent molecule upon work up.

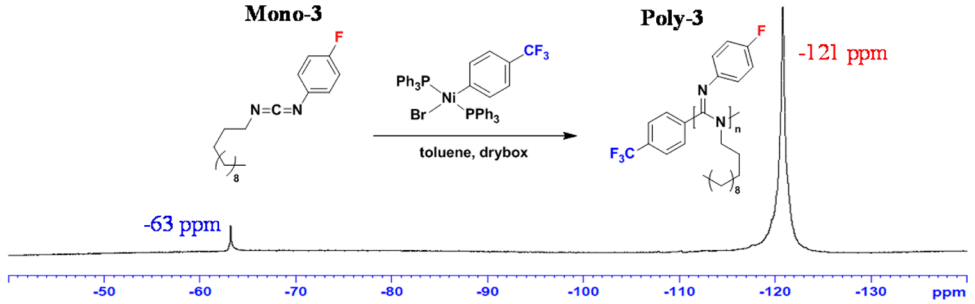

Figure 5. ^{19}F NMR of **Poly-3** polymerized using **Cat-2** (ca. [**Mono-3**]/[**Cat-2**] = 73) allowing for quantification of the average number of repeat units by relative integration of the chemical shift of the end group versus the chemical shift of the pendant group.

amplified signal-to-noise to allow for accurate measurements of M_n to compare with traditional SEC analysis. The fluorinated *N*-4-fluorophenyl-*N*′-doceylcarbodiimide (**Mono-3**) was polymerized with **Cat-2** at a wide range of monomer to catalyst ratios to form poly(*N*-4-fluorophenyl-*N*′-doceylcarbodiimide) (**Poly-3**) with a variety of molecular weights. The ^{19}F NMR spectrum of **Poly-3** (Figure 5) indeed displays two peaks with the three fluorine atoms from the 4-trifluoromethylphenyl end group visible at −63 ppm and the fluorine atom from the 4-fluorophenyl pendant group showing up at −121 ppm. The relative integration of each peak provides an accurate, quantitative determination of the average number of repeat units (n) which then can be converted to M_n.

The plot of M_n vs [**Mono-3**]/[**Cat-2**] was constructed using the M_n values measured using ^{19}F NMR and SEC to determine the level of MW control for this polymerization (Figure 6). The M_n values given by ^{19}F NMR analysis provide a nice, linear fit suggesting that the polymerization occurs in a highly controlled manner further supporting the living character of the polymerization. Additionally, the linear trendline seems to approach the origin indicating that close to all of the Ni(II) catalysts are active in the initiation process. The MW data determined by SEC for the same polymers, however, provided largely erratic results. For all tabulated M_n (^{19}F NMR and SEC), M_w (SEC), and PDI (SEC) values see the Supporting Information.

In addition to forming end-functionalized, helical polycarbodiimides, this novel polymerization technique offers the ability to generate the active initiation site *in situ* in the presence of potentially any aryl bromide offering the opportunity to functionalize a variety of candidates such as surfaces, nano-

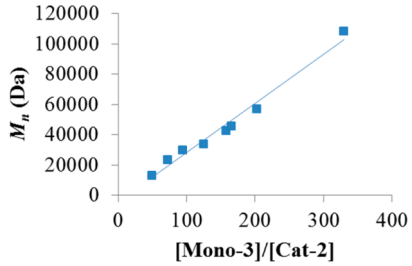

Figure 6. Plot of M_n vs [**Mono-3**]/[**Cat-2**] portraying the high degree of control over MW simply by altering the monomer-to-catalyst ratio. The M_n values were calculated using the relative intergration between the ^{19}F chemical shifts of the end group with respect to the pendant group ^{19}F chemical shifts.

particles, or single-polymer chains with rigid-rod, mesogenic polycarbodiimides. This route also may provide the potential to mechanically reinforce the typically soft, brittle nature of polycarbodiimides to broaden the range of potential applications for these interesting materials. To demonstrate this, poly(4-bromostyrene) (PBrS) was reacted with Ni(COD)$_2$ and PPh$_3$ to form the active bis(triphenylphosphino)-aryl Ni(II) bromide complex appended to the random coil polymer backbone (Scheme 2). The complex formation was apparent upon addition of the Ni(COD)$_2$ as evident by the distinct clear to orange color change as well as the appearance of ^{31}P NMR chemical shift at ca. 22.3 ppm within 1 h of addition (Figure S21). The chiral (*S*)-PEMC (**Mono-2*S***) monomer was then added to the mixture to form novel, helical-*graft*-random coil copolymers. The target was to functionalize

dx.doi.org/10.1021/ma5009429 | *Macromolecules* XXXX, XXX, XXX–XXX

Scheme 2. Synthesis of (*S*)-PPEMC-*g*-PBrS Rod−Coil Graft Copolymer by Forming the Active Ni(II) Macroinitiator Appended to ∼22% (x = 0.78; n = 48) of the Aryl Bromide Pendant Groups of PBrS

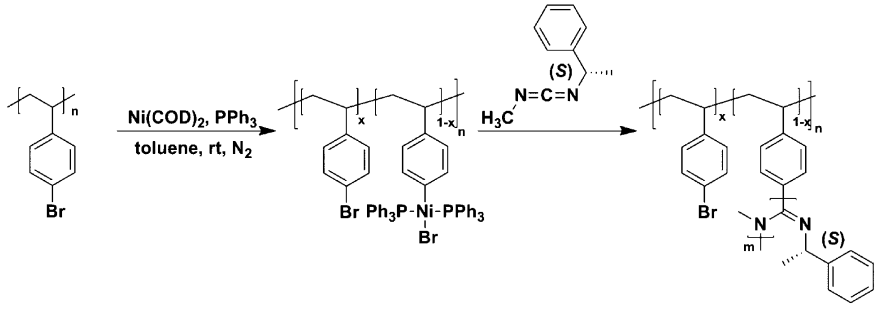

∼22% of the aryl bromide repeat units of PBrS with rod-like (*S*)-PPEMC (**Poly-2*S***) chains to study the effect of incorporating main-chain liquid crystalline grafts to conventional random-coil polymer systems. Leaving the macroinitiator solution stirring for >2 h in the absence of monomer under inert atmosphere resulted in the formation of black precipitate believed to be colloidal Ni(0) and cross-linked PBrS formed upon disproportionation giving the macroinitiator comparable stability in solution to **Cat-1** and **2**.

The grafting of (*S*)-PPEMC (**Poly-2*S***) from PBrS was monitored and confirmed by ^{1}H NMR and SEC. Similar to the homopolymerization of **Poly-2S** with **Cat-1**, the polymerization reaction was complete after ∼90 min as evident by the complete disappearance of the N═C═N stretching mode and the appearance of the C═N imine stretching mode in the IR spectra. The formation of the covalently bound (*S*)-PPEMC-*g*-PBrS was confirmed by SEC (Figure 7) with a distinct increase

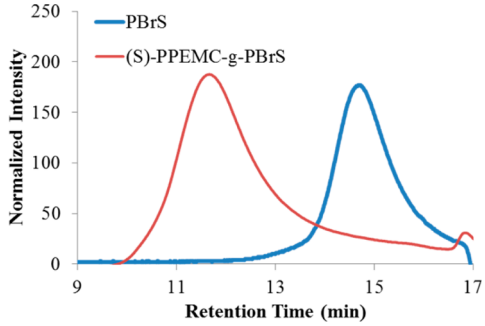

Figure 7. SEC chromatogram of parent PBrS (blue) and (*S*)-PPEMC-*g*-PBrS (red) showing distinct shift in retention time indicative of significant increases of MW upon graft copolymerization.

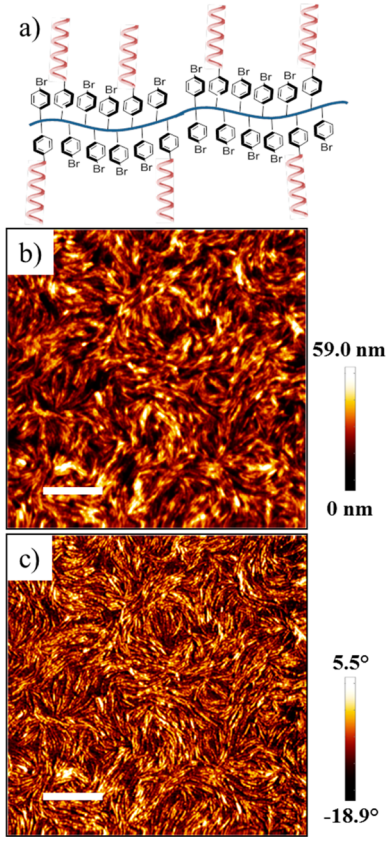

Figure 8. Cartoon representation (a), height (b), and phase (c) TMAFM micrographs of (*S*)-PPEMC-*g*-PBrS spin-coated from $CHCl_3$ and annealed in saturated $CHCl_3$ desiccator for 24 h (scan size = 15 × 15 μm; scale bar = 3 μm; RMS (roughness) = 8.54 nm).

in molecular weight and decrease in retention time from the parent PBrS sample (M_n = 8800 Da; PDI = 1.08; t = 14.7 min) to the graft copolymer (M_n = 49600 Da; PDI = 2.34; t = 11.7 min). Assuming that all available Ni(0) reagent oxidatively adds to the polymer chain, which was confirmed by ^{31}P NMR, the polymer chains should grow from ∼22% of the aryl bromide pendants based on the amount of nickel present in the system. Correlating this to the observed MW increase in SEC suggests that each PPEMC graft is, on average, 56 repeat units long (ca. M_n(PPEMC) = 8900 Da). The VCD spectra of the graft copolymer looks very similar to the homopolymer **Poly-2*S*** confirming that the same helical enantiomer is formed upon grafting (*S*)-PPEMC from PBrS (Figure S20). Thermogravametric analysis (TGA) of the graft copolymer shows a two-step degradation with the first onset of mass loss at 174 °C corresponding to the decomposition of the (*S*)-PPEMC grafts followed by the decomposition of the PBrS main chain at 385 °C (Figure S23). The relative mass loss of each segment matches very closely with the observed MW increase in SEC with ∼81% of the mass loss observed attributed to the PPEMC chains and ∼19% mass loss associated with PBrS parent polymer chain. Differential scanning calorimetry (DSC) of the graft copolymer displays one thermal transition associated with T_g of PBrS at 125 °C (Figure S22). The graft copolymerization shows no effect on T_g and no thermal transitions are typically observed for the PPEMC chains despite the crystallinity of the PPEMC homopolymers. This is believed to be due to the polymers low degradation temperature causing the polymer to thermally decompose into monomer units before any melting transition is observed.

dx.doi.org/10.1021/ma5009429 | *Macromolecules* XXXX, XXX, XXX−XXX

The DSC and TGA data can be found in the Supporting Information.

Incorporating mesogenic units into main chain random-coil polymers often results in the evolution of interesting aggregation behavior and thin film morphologies.[39,40] The thin film morphology of (*S*)-PPEMC-*g*-PBrS was investigated by spin-coating dilute solutions of the polymer (ca. 5.0 mg/mL) onto highly polished silicon wafers and annealing the thin films in a $CHCl_3$ vapor for 24 h. The lyotropic liquid crystalline properties of (*S*)-PPEMC in $CHCl_3$ solutions is one the main reasons for the use of $CHCl_3$ to study the thin film morphology of the graft copolymer.[23] The thin films were then imaged using tapping-mode atomic force microscopy (TMAFM) revealing nanofibular aggregation behavior of the graft copolymers (Figure 8). The relative diameter of a single, fully extended graft copolymer chain (from one PPEMC chain end to another) was estimated to be ∼17 nm in diameter using the experimental mass per length (M_L) and persistence length (P) values determined for (*R*)-PPEMC by Nieh et al.[41] Statistical analysis of the nanofibril aggregates provides an average diameter of 171 ± 28 nm corresponding to, on average, ∼10 polymer chains aligned from one edge of the fibril to another. To unambiguously determine the level of arrangement and spacing between polymer chains, a series of these copolymers will be synthesized and investigated by TMAFM and thin-film SA-XRD in future work. It is clear, however, that this new controlled living polymerization technique offers vast new opportunities in the incorporation of chiral, helical, rigid-rod polycarbodiimides into a variety of systems.

CONCLUSION

The rapid polymerization of carbodiimide monomers with (bistriphenylphosphino)aryl nickel(II) bromide initiators was discovered to occur in a controlled living fashion with near quantitative yields isolated in ∼90 min for the polymerization of **Mono-2**. One of the main advantages of these nickel(II) initiators compared to their titanium(IV) counterparts is their high air/moisture stability in the solid state making them much simpler to synthesize and purify. The polymerization is initiated upon aryl ligand transfer to the center carbodiimide carbon forming the active Ni(II) amidinate complex. Additional carbodiimide monomer units then insert themselves into the nickel−nitrogen bond forming a new amidinate complex and propagation ensues. Linear relationships of percent conversion vs M_n, $\ln([M]_o/[M])$ vs time, and monomer: initiator ratio vs M_n provide substantial evidence that the polymerization occurs via living chain-growth mechanism. The presence of the transferred aryl end group at the terminus of the polymer chain was also confirmed by MALDI−TOF and ^{19}F NMR providing further evidence for the proposed mechanism of polymerization. The *in situ* formation of the active Ni(II) initiator appended to the random coil polymer PBrS was also demonstrated by reacting ∼22% of the available aryl bromide pendants with $Ni(COD)_2$ and triphenylphosphine. The chiral **Mono-2*S*** was then "grafted from" the PBrS macroinitiator chain forming a new class of helical-*g*-coil copolymers with mesogenic, rigid rod polycarbodiimide segments covalently bound to the PBrS chains. This graft copolymer adopts nanofibular morphology as evident by TMAFM believed to be caused to the aggregation of the mesogenic PPEMC segments into large, fiber-like aggregates with an average diameter of 171 ± 28 nm. This novel polymerization technique offers exciting new opportunities in the facile incorporation of helical, rigid-rod polycarbodiimides into a variety of systems such as block copolymers, graft copolymers, star polymers, hybrid inorganic/organic materials, etc.

ASSOCIATED CONTENT

Supporting Information

Further experimental synthesis and characterization of all precursor compounds and polymers including NMR, IR, specific OR, and HRMS data. This material is available free of charge via the Internet at http://pubs.acs.org/.

AUTHOR INFORMATION

Corresponding Author

*(B.M.N.) E-mail: Bruce.novak@utdallas.edu.

Notes

The authors declare no competing financial interest.

ACKNOWLEDGMENTS

Funding for this work was provided by the Faculty start up fund from the University of Texas at Dallas (UTD) and the Endowed Chair for Excellence at UTD. We gratefully acknowledge the NSF-MRI grant (CHE-1126177) used to purchase the Bruker Advance III 500 NMR instrument.

REFERENCES

(1) Bunz, U. H. F. *Macromol. Rapid Commun.* **2009**, *30*, 772−805.
(2) Rehahn, M.; Schlüter, A.-D.; Wegner, G.; Feast, W. J. *Polymer* **1989**, *30*, 1060−1062.
(3) Heitz, W.; Bruegging, W.; Freund, L.; Gailberger, M.; Greiner, A.; Jung, H.; Kampschulte, U.; Niessner, N.; Osan, F.; et al. *Makromol. Chem.* **1988**, *189*, 119−127.
(4) Chen, T.-A.; Wu, X.; Rieke, R. D. *J. Am. Chem. Soc.* **1995**, *117*, 233−244.
(5) Matyjaszewski, K.; Tsarevsky, N. V. *Nat. Chem.* **2009**, *1*, 276−288.
(6) Matyjaszewski, K.; Xia, J. *Chem. Rev.* **2001**, *101*, 2921−2990.
(7) Bielawski, C. W.; Grubbs, R. H. *Prog. Polym. Sci.* **2007**, *32*, 1−29.
(8) Lynn, D. M.; Kanaoka, S.; Grubbs, R. H. *J. Am. Chem. Soc.* **1996**, *118*, 784−790.
(9) Goodwin, A.; Novak, B. M. *Macromolecules* **1994**, *27*, 5520−5522.
(10) Patten, T. E.; Novak, B. M. *Macromolecules* **1993**, *26*, 436−439.
(11) Deming, T. J.; Novak, B. M. *J. Am. Chem. Soc.* **1992**, *114*, 4400−4402.
(12) Xue, Y.-X.; Zhu, Y.-Y.; Gao, L.-M.; He, X.-Y.; Liu, N.; Zhang, W.-Y.; Yin, J.; Ding, Y.; Zhou, H.; Wu, Z.-Q. *J. Am. Chem. Soc.* **2014**, *136*, 4706−4713.
(13) Lanni, E. L.; Locke, J. R.; Gleave, C. M.; McNeil, A. J. *Macromolecules* **2011**, *44*, 5136−5145.
(14) Kim, Y.-J.; Sato, R.; Maruyama, T.; Osakada, K.; Yamamoto, T. *J. Chem. Soc., Dalton Trans.* **1994**, *0*, 943−948.
(15) Tkachov, R.; Senkovskyy, V.; Komber, H.; Sommer, J.-U.; Kiriy, A. *J. Am. Chem. Soc.* **2010**, *132*, 7803−7810.
(16) Traina, C. A.; Bakus, R. C., II; Bazan, G. C. *J. Am. Chem. Soc.* **2011**, *133*, 12600−12607.
(17) Palermo, E. F.; McNeil, A. J. *Macromolecules* **2012**, *45*, 5948−5955.
(18) Matyjaszewski, K.; Miller, P. J.; Pyun, J.; Kickelbick, G.; Diamanti, S. *Macromolecules* **1999**, *32*, 6526−6535.
(19) Khanduyeva, N.; Senkovskyy, V.; Beryozkina, T.; Bocharova, V.; Simon, F.; Nitschke, M.; Stamm, M.; Groetzschel, R.; Kiriy, A. *Macromolecules* **2008**, *41*, 7383−7389.
(20) Smeets, A.; Van den Bergh, K.; De Winter, J.; Gerbaux, P.; Verbiest, T.; Koeckelberghs, G. *Macromolecules* **2009**, *42*, 7638−7641.
(21) Kreutzer, G.; Ternat, C.; Nguyen, T. Q.; Plummer, C. J. G.; Mnson, J.-A. E.; Castelletto, V.; Hamley, I. W.; Sun, F.; Sheiko, S. S.;

Herrmann, A.; Ouali, L.; Sommer, H.; Fieber, W.; Velazco, M. I.; Klok, H.-A. *Macromolecules* **2006**, *39*, 4507−4516.
(22) Senkovskyy, V.; Tkachov, R.; Beryozkina, T.; Komber, H.; Oertel, U.; Horecha, M.; Bocharova, V.; Stamm, M.; Gevorgyan, S. A.; Krebs, F. C.; Kiriy, A. *J. Am. Chem. Soc.* **2009**, *131*, 16445−16453.
(23) Kim, J.; Novak, B. M.; Waddon, A. J. *Macromolecules* **2004**, *37*, 8286−8292.
(24) Kim, J.; Novak, B. M.; Waddon, A. J. *Macromolecules* **2004**, *37*, 1660−1662.
(25) Schlitzer, D. S.; Novak, B. M. *J. Am. Chem. Soc.* **1998**, *120*, 2196−2197.
(26) Budhathoki-Uprety, J.; Novak, B. M. *Polymer* **2010**, *51*, 2140−2146.
(27) Tang, H.-Z.; Novak, B. M.; He, J.; Polavarapu, P. L. *Angew. Chem., Int. Ed.* **2005**, *44*, 7298−7301.
(28) Tang, H.-Z.; Lu, Y.; Tian, G.; Capracotta, M. D.; Novak, B. M. *J. Am. Chem. Soc.* **2004**, *126*, 3722−3723.
(29) Kennemur, J. G.; Clark, J. B.; Tian, G.; Novak, B. M. *Macromolecules* **2010**, *43*, 1867−1873.
(30) Reuther, J. F.; Novak, B. M. *J. Am. Chem. Soc.* **2013**, *135*, 19292−19303.
(31) DeSousa, J. D.; Novak, B. M. *ACS Macro Lett.* **2012**, *1*, 672−675.
(32) Hidai, M.; Kashiwagi, T.; Ikeuchi, T.; Uchida, Y. *J. Organomet. Chem.* **1971**, *30*, 279−282.
(33) Otsuka, S.; Nakamura, A.; Yoshida, T.; Naruto, M.; Ataka, K. *J. Am. Chem. Soc.* **1973**, *95*, 3180−3188.
(34) Ge, S.; Hartwig, J. F. *J. Am. Chem. Soc.* **2011**, *133*, 16330−16333.
(35) De Brouwer, H.; Schellekens, M. A. J.; Klumperman, B.; Monteiro, M. J.; German, A. L. *J. Polym. Sci., Part A: Polym. Chem.* **2000**, *38*, 3596−3603.
(36) Reuther, J. F.; DeSousa, J. D.; Novak, B. M. *Macromolecules* **2012**, *45*, 7719−7728.
(37) Tang, H.-Z.; Garland, E. R.; Novak, B. M.; He, J.; Polavarapu, P. L.; Sun, F. C.; Sheiko, S. S. *Macromolecules* **2007**, *40*, 3575−3580.
(38) Merten, C.; Reuther, J. F.; DeSousa, J. D.; Novak, B. M. *Phys. Chem. Chem. Phys.* **2014**, *16*, 11456−11460.
(39) Fischer, H.; Poser, S. *Acta Polym.* **1996**, *47*, 413−428.
(40) Poser, S.; Fischer, H.; Arnold, M. *Prog. Polym. Sci.* **1998**, *23*, 1337−1379.
(41) Nieh, M.-P.; Goodwin, A. A.; Stewart, J. R.; Novak, B. M.; Hoagland, D. A. *Macromolecules* **1998**, *31*, 3151−3154.